

RESEARCH

Frequent *SLC12A3* mutations in Chinese Gitelman syndrome patients: structure and function disorder

Lanping Jiang^{1,2,*}, Xiaoyan Peng^{1,3,*}, Bingbin Zhao¹, Lei Zhang¹, Lubin Xu¹, Xuemei Li¹, Min Nie⁴ and Limeng Chen¹¹Department of Nephrology, State Key Laboratory of Complex Severe and Rare Diseases, Peking Union Medical College Hospital, Chinese Academy of Medical Sciences and Peking Union Medical College, Beijing, China²Department of Nephrology & Key Laboratory of Nephrology, National Health Commission and Guangdong Province, The First Affiliated Hospital, Sun Yat-sen University, Guangzhou, China³Renal Division, Children's Hospital Affiliated to Capital Institute of Pediatrics, Beijing, China⁴Department of Endocrinology & Key Laboratory of Endocrinology, National Health and Family Planning Commission, Chinese Academy of Medical Sciences and Peking Union Medical College, Beijing, ChinaCorrespondence should be addressed to L Chen or M Nie: chenlimeng@pumch.cn or nm_pumch@aliyun.com

*(L Jiang and X Peng contributed equally to this work)

Abstract

Purposes: This study was conducted to identify the frequent mutations from reported Chinese Gitelman syndrome (GS) patients, to predict the three-dimensional structure change of human Na–Cl co-transporter (hNCC), and to test the activity of these mutations and some novel mutations *in vitro* and *in vivo*.

Methods: *SLC12A3* gene mutations in Chinese GS patients previously reported in the PubMed, China National Knowledge Infrastructure, and Wanfang database were summarized. Predicted configurations of wild type (WT) and mutant proteins were achieved using the I-TASSER workplace. Six missense mutations (T60M, L215F, D486N, N534K, Q617R, and R928C) were generated by site-directed mutagenesis. ²²Na⁺ uptake experiment was carried out in the *Xenopus laevis* oocyte expression system. In the study, 35 GS patients and 20 healthy volunteers underwent the thiazide test.

Results: T60M, T163M, D486N, R913Q, R928C, and R959frameshift were frequent *SLC12A3* gene mutations (mutated frequency >3%) in 310 Chinese GS families. The protein's three-dimensional structure was predicted to be altered in all mutations. Compared with WT hNCC, the thiazide-sensitive ²²Na⁺ uptake was significantly diminished for all six mutations: T60M 22 ± 9.2%, R928C 29 ± 12%, L215F 38 ± 14%, N534K 41 ± 15.5%, Q617R 63 ± 22.1%, and D486N 77 ± 20.4%. In thiazide test, the net increase in chloride fractional excretion in 20 healthy controls was significantly higher than GS patients with or without T60M or D486N mutations.

Conclusions: Frequent mutations (T60M, D486N, and R928C) and novel mutations (L215F, N534K, and Q617R) lead to protein structure alternation and protein dysfunction verified by ²²Na⁺ uptake experiment *in vitro* and thiazide test on the patients.

Key Words

- ▶ Gitelman syndrome
- ▶ *SLC12A3* gene
- ▶ frequent mutations
- ▶ ²²Na⁺ uptake activity
- ▶ Thiazide test

Endocrine Connections
(2022) 11, e210262

Introduction

Gitelman syndrome (GS, OMIM263800) is a recessively inherited salt-losing tubulopathy caused by mutations of *SLC12A3* gene, which encodes the thiazide-sensitive human Na–Cl co-transporter (hNCC NM_000339.2; OMIM 600968) (1, 2). More than 500 *SLC12A3* gene mutations were found previously (<http://www.hgmd.cf.ac.uk/ac/index.php>), and some frequent mutations were identified in Chinese, Japanese, and European patients (3, 4, 5, 6, 7, 8, 9). Different frequent mutations of different populations indicate location and ancestral diversity of *SLC12A3* gene mutation (3, 8). In different studies of Chinese GS patients (3, 4, 6, 10, 11), T60M, D486N, R913Q, and R928C were reported as the frequent mutations, which were consistent with our previous studies (12, 13, 14, 15, 16, 17, 18). Even though the functional impact of mutations on NCC proteins could be confirmed in the *Xenopus laevis* oocyte expression system *in vitro* (1, 7, 19, 20, 21, 22, 23) and GS mimic mouse models (24, 25) and thiazide test (13, 17, 26, 27) *in vivo*, the functional characteristics of the most frequent NCC mutations and novel mutations of Chinese patients remain unknown. Few studies integrate the protein configurations with the function of hNCC mutations *in vitro* and *in vivo*. Herein, this study was conducted to summarize all reported *SLC12A3* gene mutations in Chinese GS patients and our 105 cases, to identify the most frequent ones, to predict the protein configurations, and to test the activity of these mutations *in vitro* and *in vivo*.

Materials and methods

The study protocol was approved by the Ethics Committee on Human Studies at Peking Union Medical College Hospital (PUMCH), Chinese Academy of Medical Sciences and Peking Union Medical College, Beijing, China. The authors adhered to the Declaration of Helsinki, and patients of our hospital were included after providing their informed consent.

Patient recruitment and mutation analysis of *SLC12A3* gene

This study was based on the GS cohort that was reported in our previous studies (12, 13, 14, 15, 16, 17, 18). From 2004, hypokalemic patients who presented to Peking Union Medical College Hospital with potassium loss from the kidney, metabolic alkalosis, and normotension were included. *SLC12A3* gene screening was performed to

confirm the diagnosis of GS. The method of *SLC12A3* gene direct sequencing was elaborated in our previous studies (12, 13). The most frequent mutations of the *SLC12A3* gene in Chinese patients were identified as follows. PubMed, China National Knowledge Infrastructure, and Wanfang databases (Academic Search Engines for Chinese manuscripts) were searched with the keyword ‘Gitelman syndrome’ up to August 2019, and all the literature published by Chinese researchers (with individual patient’s gene mutations available) were included. The same patient repeatedly reported in different articles by the same group was only counted once. Those studies that included apparent mistakes without reasonable explanation were excluded. Together with the mutations found in our laboratory, we calculated the type and number of mutated alleles. To avoid repetitive calculations, a heterozygous mutated allele that occurred in one family was counted only once and a homozygous mutated allele was counted twice. We defined the mutated allele, whose frequency was greater than 3%, as a frequent mutation.

Configuration prediction of WT and mutant hNCC proteins

Predicted three-dimensional structures of WT and mutant proteins were achieved using the iterative threading assembly refinement (I-TASSER) workplace (<https://zhanglab.ccmb.med.umich.edu/I-TASSER/>) (28, 29). WT and nine mutant protein amino acid sequences (T60M, T163M, L215F, D486N, N534K, Q617R, R913Q, R928C, and R959frameshift) were sent to I-TASSER. The I-TASSER system used C-score to evaluate the accuracy of the models, C-score was typically in the range of (–5, 2); a higher value signified a model with more confidence and vice-versa (28). The model with highest C-score was chosen. The effect of mutations on protein configurations of NCC was visualized using PyMOL Viewer.

Construction of WT and mutated hNCC cDNA

Human renal total RNA was isolated from the paracancerous tissue collected from patients undergoing nephrectomy due to renal cancer by TRIzol[®] RNA extraction method (Life Technologies). The first strand of cDNA was generated according to the Reverse Transcription system manual (Promega). The hNCC cDNA was obtained by PCR with the forward primer 5’-ATGGCAGAACTGCCACAACAGAGAC-3’ and the reverse primer 5’-TTACTGGCAGTAAAAGGTGAGCACG-3’. Then, the hNCC cDNA was cloned into a PGEM-T vector (Promega). Three frequent mutations (T60M, D486N, and

R928C) and three novel mutations (L215F, N534K, and Q617R) were introduced into the hNCC-pGEM T vector by site-directed mutagenesis kit (TransGene, Beijing, China). The WT and mutant hNCC cDNA pGEM T vectors were confirmed by DNA direct sequencing.

Xenopus laevis oocyte transport assay

As described in previous studies (30, 31, 32, 33), human *SLC12A3* cRNA mutant variants were prepared by *in vitro* transcription reaction utilizing the T7 or SP6 mMessage mMachine (Ambion). Freezing *X. laevis* oocytes (stages V and VI) were obtained from the lab of National Institute of Diabetes and Digestive and Kidney Diseases, National Institutes of Health Bethesda, MD, USA). They were transferred to calcium-containing OR-2 (1 mM CaCl₂) and maintained at 18–20°C until injected with cRNA. Oocytes were injected utilizing a Nanoject II injector (Drummond Scientific, Broomall, PA, USA). Injection volumes were 36.8 nL and cRNA concentrations were 1 ng/nL. Sham-injected oocytes were injected with 36.8 nL of water. After injection, the oocytes were maintained in calcium-containing OR-2 at 18–20°C until the experiments were performed.

Three days post-injection, the oocytes were transferred to Cl⁻-free ND96 medium (96 mM Na⁺- isethionate, 2 mM K⁺-gluconate, 1.8 mM Ca²⁺-gluconate, 1 mM Mg²⁺-gluconate, 5 mM Hepes, pH 7.4, 2.5 mM sodium pyruvate, and 5 mg/100 mL gentamicin) for 24 h. To begin uptake experiments, the oocytes were incubated in Cl⁻-free ND96 medium containing 1 mM ouabain, 0.1 mM amiloride, and 0.1 mM bumetanide for 30 min, following specified times (0.5–2 h) of uptake in K⁺-free NaCl medium (40 mM NaCl, 56 mM sodium gluconate, 4 mM CaCl₂, 1 mM MgCl₂, and 5 mM Hepes/Tris, pH 7.4) containing 1 mM ouabain, 0.1 mM amiloride, 0.1 mM bumetanide, and 1 μCi/mL ²²Na⁺. After incubation at room temperature, the oocytes were washed four times with ice-cold PBS. Individual oocytes per replicate were solubilized with 10% SDS, and internalized radioactivity was quantified by Automatic Gamma Counter (Perkin Elmer) as nmol/oocyte. Each data point represents the mean value of 10–15 oocytes. Each experiment was repeated a minimum of three times with similar results.

Thiazide test

Thiazide tests were performed according to the standard protocol as previously described (13, 14, 17, 18). Thirty-five of our 105 GS patients signed the consent form and participated in the thiazide test. Twenty healthy volunteers underwent the thiazide test as well.

Statistical analysis

Normally distributed variables were expressed as the mean ± s.d. and were compared using unpaired *t*-tests. The differences in thiazide tests between healthy volunteers and each subgroup of GS patients were compared using unpaired *t*-tests. One-way ANOVA was performed to evaluate the thiazide test differences among three subgroups of GS patients, followed by least significant difference *post hoc* test for each two subgroups. Differences were considered significant when *P* < 0.05. All statistical analyses were performed with the statistical software 17.0 (SPSS).

Results

The frequent mutations of Chinese GS patients

A total of 105 GS patients from 101 non-consanguineous Chinese families in PUMCH were recruited in this study. Sixty-nine mutations, including 20 novel mutations, were identified in this cohort. In total, 83 papers were utilized in the study (Supplementary Table 1, see section on [supplementary materials](#) given at the end of this article). As shown in Fig. 1, 155 *SLC12A3* gene mutations were detected in 338 Chinese GS patients from 310 unrelated families, including 112 missense mutations, 9 nonsense mutations, 11 splicing mutations, 16 small deletions, 3 small insertions, 3 small indels, and 1 gross deletion. One patient carried five mutant sites (one homozygous nonsense mutation and three heterozygous missense mutations). Five patients, including two patients with two homozygous mutations and three patients with one homozygous mutation and two heterozygous mutations, carried four mutant sites. Twenty-seven patients carried three mutant sites. One hundred seventy-three patients carried compound heterozygous mutations. Fifty-six patients carried homozygous mutations. Seventy-six patients carried single heterozygous mutations.

Figure 2 shows the frequency and distribution of the 155 mutations. The mutations were distributed in 25 of 26 exons and their flanking intronic regions (except exon 19). T60M, T163M, D486N, R913Q, R928C, and R959frameshift were found to be the frequent mutations (mutated allele frequency greater than 3%). T60M was the most frequent mutation in the Chinese GS patients, with 75 mutated alleles (12.7%). The second most frequent mutation was D486N detected in 52 of all 591 mutated alleles (8.8%), followed by the mutant alleles of R913Q (3.9%), R928C (3.6%), T163M (3.2%), and R959frameshift (3.2%). These six mutations accounted for 35.4% of all 591 mutated alleles.

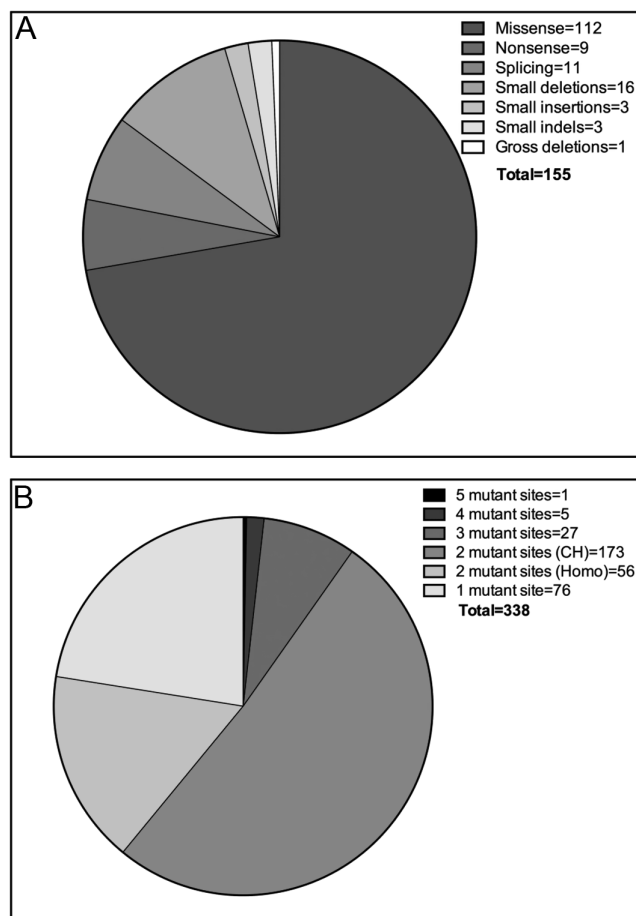


Figure 1
Number of different mutation types found in Chinese GS patients (A) and the number of mutant sites detected in each patient (B). (A) A total of 155 *SLC12A3* gene mutations were detected in 338 Chinese GS patients from 310 unrelated families, including 112 missense mutations (72.3%), 9 nonsense mutations (5.8%), 11 splicing mutations (7.1%), 16 small deletions (10.3%), 3 small insertions (1.9%), 3 small indels (1.9%), and 1 gross deletion (0.6%). (B) Five mutant sites were detected in 1 patient, 4 mutant sites were found in 5 patients, 3 mutant sites were carried by 27 patients, 2 mutant sites (compound heterozygous, CH) were detected in 173 patients, 2 mutant sites (homozygous, Homo) were found in 56 patients, and single heterozygous mutation was carried by 76 patients.

Configuration prediction of WT and nine mutant hNCC proteins

The C-score results of five models of WT hNCC and nine mutations predicted by I-TASSER system are shown in Supplementary Table 2. The configuration of six frequent mutations (T60M, T163M, D486N, R913Q, R928C, and R959frameshift) is presented in Fig. 3, and the predicted structure of three novel mutations found in our early admitted GS patients (L215F, N534K, and Q617R) are shown in Supplementary Fig. 1. In the WT configuration, there was no β -sheet structures, which were found in the C-terminus of all mutations. The predicted secondary

structure of the 60th residue was changed from loop of WT threonine (Fig. 3A) to an α -helix of methionine mutation (Fig. 3A'); similarly, in the 215th residue, leucine mutated to phenylalanine (Supplementary Fig. 1A and A'). When the 163th residue threonine mutated to methionine, the end of the first transmembrane α -helix changed from A166 to Q165, and the beginning of the second transmembrane α -helix transformed from V169 to I168 subsequently (Fig. 3B and B'). On the WT hNCC protein configuration, 913th residue arginine was between two α -helices. When it mutated to glutamine, it was located between a β -sheet and an α -helix (Fig. 3D and D'). R959frameshift was the mutation effect of c.2877_2878delAG, and this mutation was predicted to change the amino acids 959–968 and result in a premature stop codon at amino acid 969, leading to a truncated protein (Fig. 3F and F').

²²Na⁺ uptake activity of six missense mutations

We selected three missense mutations of the six frequent mutations and three novel mutations detected in our early admitted GS patients to test the ²²Na⁺ uptake activity. The sequence of six missense mutations (T60M, L215F, D486N, N534K, Q617R, and R928C) are presented in Fig. 4. The localization of each selected mutation on the predicted topology of hNCC is shown in Fig. 5A. T60M was an important phosphorylation site located within the N-terminus, L215F was positioned on the edge of the third transmembrane segment, D486N was located in the fourth intracellular loop, N534K was a transmembrane mutation, and Q617R and R928C were located in the C-terminus.

²²Na⁺ uptake rates were demonstrated in Fig. 5B and C. WT hNCC transported ²²Na⁺ robustly, whereas sham injections lacked activity. In comparison with WT hNCC (100 ± 12.6%), the thiazide-sensitive ²²Na⁺ uptake was significantly diminished for all mutants (T60M 22 ± 9.2%, R928C 29 ± 12%, L215F 38 ± 14%, N534K 41 ± 15.5%, Q617R 63 ± 22.1%, and D486N 77 ± 20.4%) (percentage of the ²²Na⁺ transport capacity of WT) (Fig. 5B). Furthermore, 100 μ M metolazone (a hNCC blocker) inhibited the uptake of ²²Na⁺ in WT and mutant hNCC-expressing oocytes to background levels observed in sham injections (data were not shown). The rates of NCC mutants-mediated ²²Na⁺ uptake were lower than ²²Na⁺ transport capacity of WT at every time point (0.5–2 h), but the metolazone-sensitive ²²Na⁺ uptake by WT and NCC mutants was all linear up for 2 h of incubation (Fig. 5C), which indicated better specificity between the transport activity and the genetic mutation.

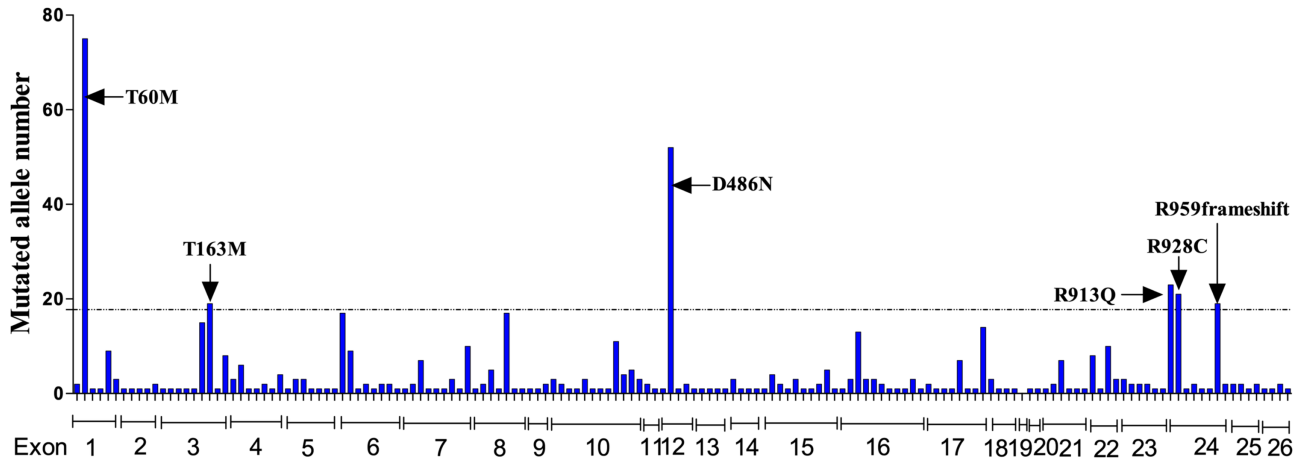


Figure 2

Frequency and distribution of the 155-detected mutations and 591-mutated alleles. A total of 338 Chinese patients from 310 unrelated families were diagnosed by *SLC12A3* gene sequencing, and 155 mutations and 591 mutated alleles were detected in these families. T60M, T163M, D486N, R913Q, R928C, and R959frameshift were the most frequent mutations (mutated allele frequency greater than 3%). On the horizontal axis, each bar represents one mutation (there is no relationship with the actual position in the exon). The dotted line corresponds to an allele frequency of 3% ($n = 17.73$).

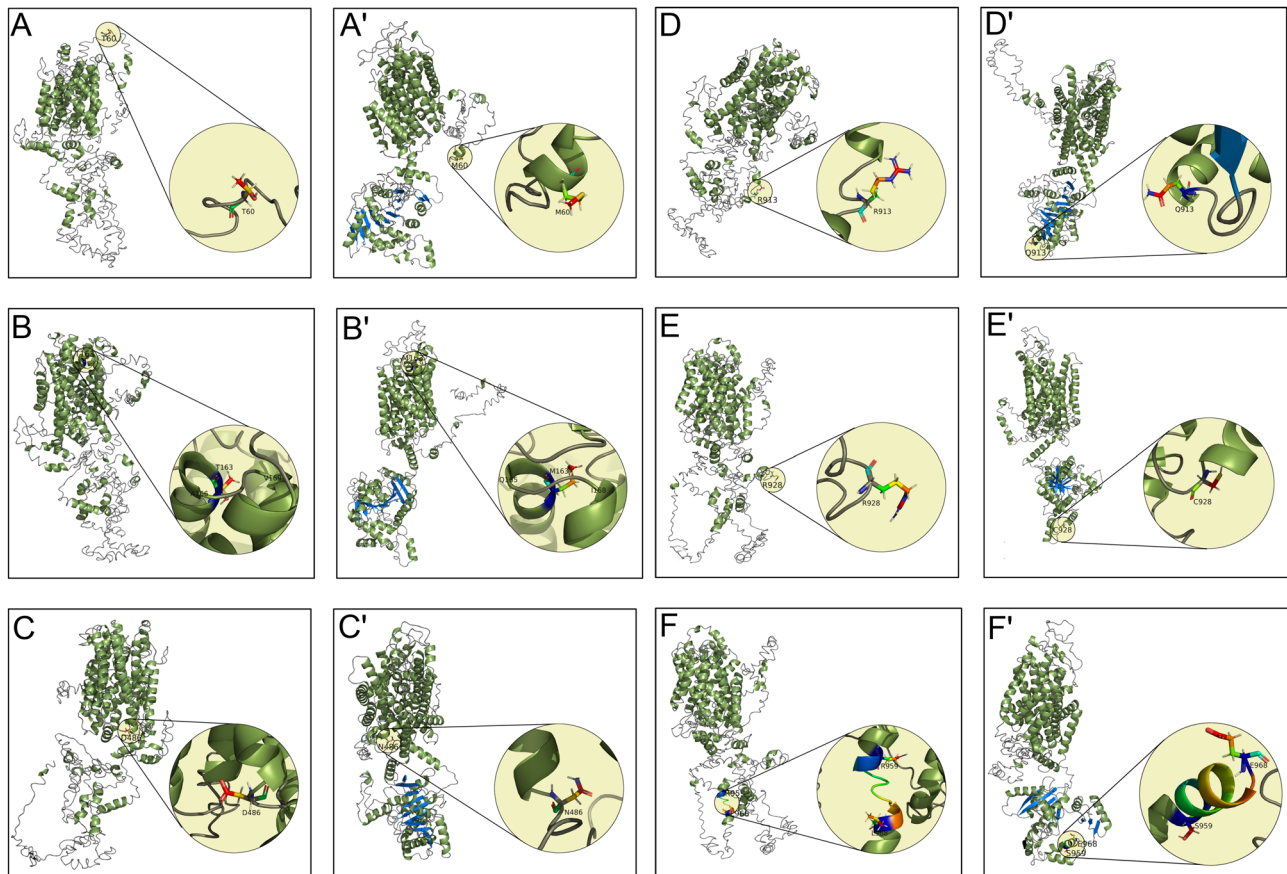
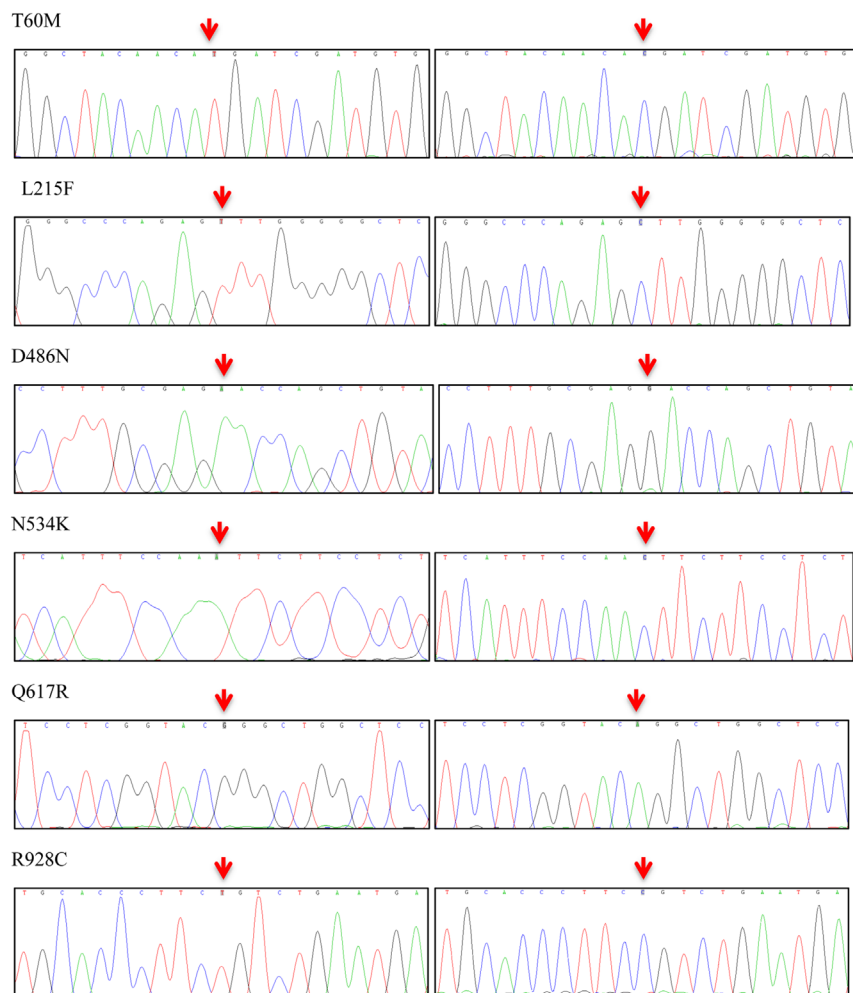


Figure 3

Predicted configuration of WT and six frequent mutant hNCC proteins. Figures A–F are configurations of WT hNCC proteins with local amplification of T60 (A), T163 (B), D486 (C), R913 (D), R928 (E), and R959 (F). Figure A'–F' are the configurations of corresponding mutant hNCC proteins with local amplification of M60 (A'), M163 (B'), N486 (C'), Q913 (D'), C928 (E'), and 959frameshift (F').

**Figure 4**

DNA sequence results of six mutated hNCC-pGEM T vectors. The DNA sequence results of six mutated hNCC-pGEM T vectors (T60M, L215F, D486N, N534K, Q617R, and R928C). The mutations' sequence results are listed at the left column and the corresponding sites of WT are presented at the right column. The sites of mutations are denoted by red arrows.

Thiazide test

The thiazide test results are presented in Fig. 6, the net increase in chloride fractional excretion (FECl) in 20 healthy controls of our previous study was $4.46 \pm 1.04\%$ (13, 17), which was significantly higher than the three subgroups of GS patients. The net increase in FECl after thiazide application in 3 GS patients with T60M mutation was $2.07 \pm 0.62\%$, in 7 GS patients with D486N mutation was $1.13 \pm 1.19\%$, and in 25 GS patients without any T60M or D486N mutation was $0.92 \pm 1.09\%$. No apparent difference was found among the subgroups.

Discussion

In this study, among 338 Chinese GS patients from 310 unrelated families, T60M, T163M, D486N, R913Q, R928C, and R959frameshift were proved to be the frequent *SLC12A3* gene mutants with altered protein's three-dimensional

structure. Notable dysfunction of the mutated hNCC protein was confirmed by $^{22}\text{Na}^+$ uptake experiment carried out in the *X. laevis* oocyte expression system and thiazide test in GS patients. It was the first time integrating the genetic mutation, hNCC protein structure and function *in vitro* and *in vivo*, which might facilitate the understanding of the genetic features of Chinese GS patients, as well as correlate the genotype with phenotype of GS.

Until now, more than 500 *SLC12A3* gene mutations have been found in GS patients of different ethnicity. In this study, we proved that T60M, D486N, T163M, R913Q, R928C, and R959frameshift were the frequent *SLC12A3* gene mutations in the largest sample of Chinese GS patients ($n=338$), published by Chinese investigators on PubMed and Chinese databases. It was consistent with the results of several previous studies, including the mutations of T60M, T163M, D486N, S710X, R871H, R913Q, R928C, R959frameshift, IVS13-191C>T, and IVS21+253C>T (Table 1) (3, 4, 6, 10, 11, 18). T60M, L858H, and R642C were found to be the frequent mutations in Japanese articles (8, 9). Eight

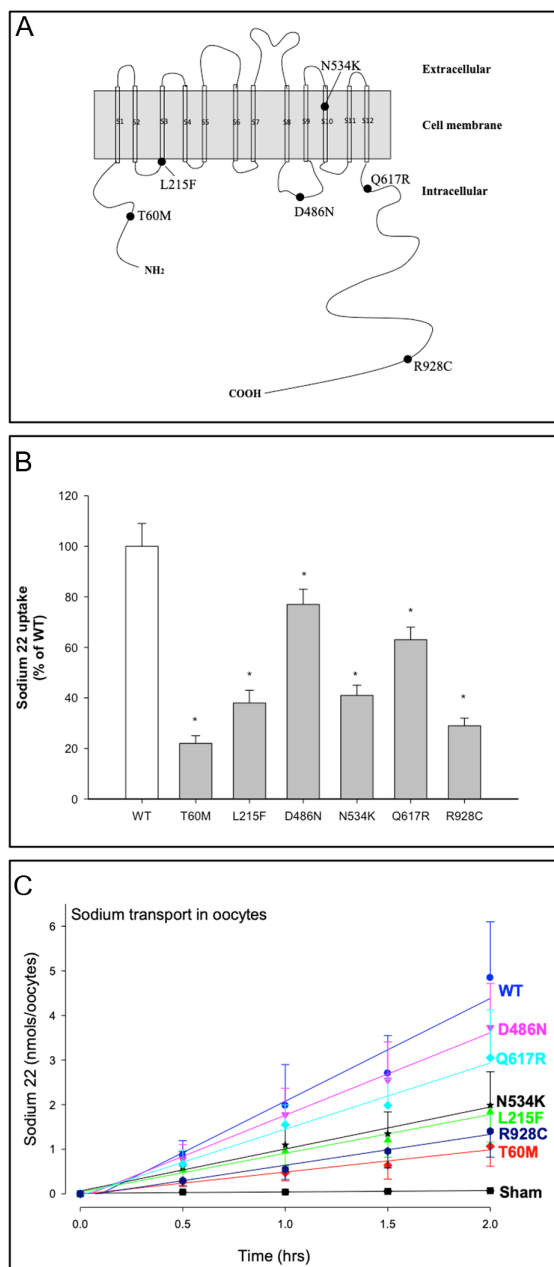


Figure 5

Location of the six studied *SLC12A3* mutations in the predicted hNCC protein and the result of $^{22}\text{Na}^+$ uptake experiment. (A) The schematic topological representation of hNCC consists of the intracellular N- and C-terminal domains and 12 transmembrane segments. We studied the function of the mutations labeled T60M, L215F, D486N, N534K, Q617R, and R928C. (B) Metolazone-sensitive $^{22}\text{Na}^+$ uptake was measured in oocytes injected with H_2O , WT (open bars), or mutant *SLC12A3* cRNAs (black bars). The uptake values are shown as percentages of WT $^{22}\text{Na}^+$ transport (WT was set as 100%). (C) Time course of $^{22}\text{Na}^+$ uptake in WT and hNCC mutant-injected *X. laevis* oocytes. *X. laevis* oocytes were microinjected with the following *SLC12A3* cRNAs: WT, sham, and mutants T60M, L215F, D486N, N534K, Q617R, and R928C. Data were presented as the mean \pm s.e.m. and compared using unpaired *t*-tests. **P* < 0.05 indicates a significant difference compared with WT *SLC12A3*-injected oocytes. Each data point represents the mean value of 10–15 oocytes.

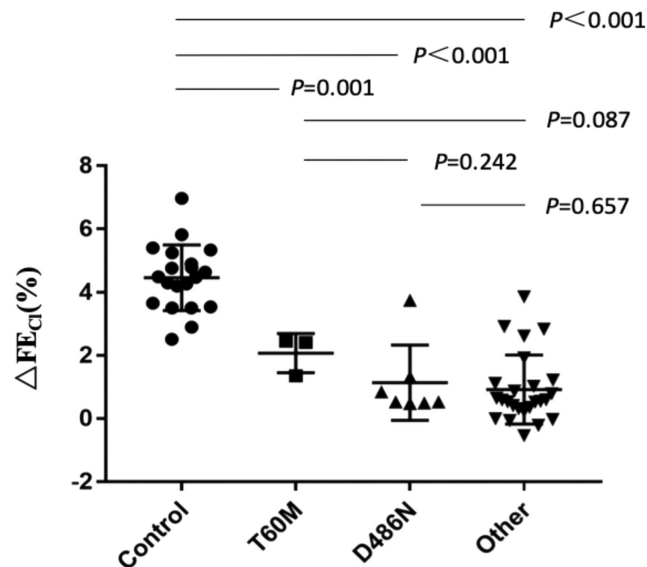


Figure 6

The thiazide test result verified hNCC dysfunction in GS patients, while no apparent difference was found among the GS patients with or without T60M or D486N mutation. The net increase in chloride fractional excretion (FECl) undergoing thiazide test in 20 healthy controls ($4.46 \pm 1.04\%$), 3 GS patients with T60M mutation ($2.07 \pm 0.62\%$), 7 GS patients with D486N mutation ($1.13 \pm 1.19\%$), and 25 GS patients without any T60M or D486N mutation ($0.92 \pm 1.09\%$). One-way ANOVA was performed to evaluate the differences among three subgroups of GS patients, followed by least significant difference *post hoc* test for each two subgroups. The differences in thiazide test between healthy volunteers and each subgroup of GS patients were compared using unpaired *t*-tests.

frequent mutations – L272P, A313V, c.1180+1G>T, G741R, L859P, R861C, c.2883+1G>T, and C994Y – were identified in two large genetically diagnosed European GS patients cohorts (5, 7). None of the European GS patients' frequent mutations were identical with the hotspot mutations in Chinese or Japanese GS patients, indicating that the distribution of *SLC12A3* gene mutations may differ from the location and ethnicities.

To our limited knowledge, we first integrally predicted the configuration alternation and investigated function change of the frequent mutations in the *SLC12A3* gene. Both the change of secondary structure and three-dimensional structures were predicted to be altered in four frequent mutations (T60M, T163M, R913Q, and R959frameshift), as well as in the novel mutation – L215F. The visible differences in the whole protein configuration caused by base substitution or bases deletion indicated these mutation were pathogenic. Among the six frequent mutations, T60 was an important phosphorylation site, and was very important for the membrane expression of hNCC and phosphorylation of the adjacent T46 and T55 sites (24). D486N was located in the fourth intracellular loop, and the mutation effect was not well-studied. R928C

Table 1 Frequent mutations in published papers and this study.

Author (reference number)	Number of GS patients	Frequent mutations	Country or district (published year)
Maki <i>et al.</i> (8)	7	T60M	Japan (2004)
Qin <i>et al.</i> (10)	13	T60M	China (2009)
Vargas-Poussou <i>et al.</i> (5)	396	A313V, c.1180+1G>T, G741R, L859P, R861C, c.2883+1G>T, and C994Y	European countries (2011)
Glaudemans <i>et al.</i> (7)	163	L272P, G741R, and c.2883+1G>T	The Netherland and other European countries (2012)
Tseng <i>et al.</i> (6)	117	R959frameshift, T60M, T163M, S710X, IVS13-191C>T, R871H, and IVS21+253C>T	China (2012)
Jiang <i>et al.</i> (18)	125 families	T60M, D486N, and R913Q	China (2015)
Wang <i>et al.</i> (4)	42	D486N	China (2016)
Ma <i>et al.</i> (3)	49	T60M and D486N	China (2016)
Zeng <i>et al.</i> (11)	133	T60M, D486N, R913Q, and R928C	China (2019)
Fujimura <i>et al.</i> (9)	185	L858H and R642C	Japan (2019)
This study	310 families	T60M, T163M, D486N, R913Q, R928C, and R959frameshift	China

(SNP rs12708965) was reported as a polymorphism, but it was believed to be deleterious and considered disease-causing (34). The sodium and chloride transport ability of these mutant hNCC proteins remains to be determined. Herein, we constructed six missense mutant hNCC, including three frequent mutations (T60M, D486N, and R928C) and three novel mutations (L215F, N534K, and Q617R) and assessed their function status directly by $^{22}\text{Na}^+$ uptake experiments on the *X. laevis* oocyte expression system *in vitro*. Compared with WT hNCC protein, $^{22}\text{Na}^+$ uptake capacity of the six mutant proteins varied from 22 to 77%, which may explain diversity in clinical presentation in GS patients. Regarding the *in vitro* functional study of NCC, a few NCC variants were studied by *X. laevis* oocyte system previously (1, 7, 19, 20, 21, 22).

As a monogenic disease, many studies tried to correlate phenotype to genotype (1, 3, 6, 10, 12, 35). Riveira-Munoz *et al.* reported that genotype and gender may determine the clinical severity in their cohort of GS patients (1). In addition, our previous study found that serum magnesium level may indicate the severity of clinical presentation (12). T60M and D486N were top two hotspot mutations in Chinese GS patients, and the result of the *in vitro* experiment illustrated apparent function difference between them. With regard to the *in vivo* functional investigation of NCC, two mouse models were generated to mimic the GS pathophysiological procedure (24, 25), and the thiazide test also determined the patient's hNCC function status directly (13, 14, 17, 26, 27, 36, 37, 38). Herein, we compared the thiazide test result among our GS patients with or without T60M or D486N mutations. However, till now, no obvious difference was observed among the three subgroups of GS patients. The inconsistency between $^{22}\text{Na}^+$ uptake experiment *in vitro* and thiazide test *in vivo*

may be caused by small sample size, limitation of *in vitro* experiment and genetic heterogeneity. The expression and function of hNCC protein may be influenced by epigenetic modifications and silent polymorphisms (1). More severe phenotype was observed in male patients compared with their female siblings who carried the same mutations (1, 35, 39). However, no significant difference was found in thiazide test result between male and female GS patients in this study. T60M carriers in Han populations have markedly lower blood pressure and slightly higher fasting plasma glucose compared with normal controls (40).

Although we tried to summarize all reported Chinese GS patients' mutations, there were still three studies excluded as the individual mutations were unavailable (4, 6, 41), and this result may cause deviation in the calculation of mutation frequency. In addition, 76 of 338 Chinese GS patients (22.5%) were only detected with single heterozygous mutation, and the percentage of single heterozygous mutation patient in other large cohort studies varied from 9.4 to 22.6% (5, 6, 7, 11). More mutations may be detected if multiplex ligation-dependent probe amplification can be used to search for large rearrangements. Whether there is clinical presentation difference between these single heterozygous mutation GS patients and other GS patients need further study. More GS patients with only T60M or D486N mutation participating in the thiazide test may help us to better understand phenotype-genotype correlation of this disease.

In conclusion, we first integrally proved the protein structure alternation, as well as $^{22}\text{Na}^+$ uptake experiment *in vitro* and thiazide test on patients verified the dysfunction of mutated hNCC proteins, in Chinese GS patients with frequent mutations (T60M, D486N, and R928C) and novel mutations (L215F, N534K, and Q617R). Future studies are

needed to reveal the underlying pathogenic mechanism in GS and to evaluate the phenotype–genotype correlations to improve the prognosis of GS.

Supplementary materials

This is linked to the online version of the paper at <https://doi.org/10.1530/EC-21-0262>.

Declaration of interest

The authors declare that there is no conflict of interest that could be perceived as prejudicing the impartiality of the research reported.

Funding

This work was partially supported by grants from the Beijing Natural Science Foundation (L202035 to C L); Capital's Funds for Health Improvement and Research (CFH 2020-2-4018 to C L); the National Natural Scientific Foundation of China (81970607, 81470937 to C L and 81600545 to J L); the Key Research and Development Program of Ningxia Hui Autonomous Region (2018BFG02010 to C L); CAMS Innovation Fund for Medical Sciences (CIFMS 2020-I2M-C and T-A-001 to C L); the Capital Specialized Clinical Application Project (Z171100001017196 to C L); Chinese Academy of Medical Sciences Innovation Fund for Medical Sciences (CIFMS 2016-I2M-2-004 to C L); National Key-point Research Program Precision Medicine Grant (2016YFC0901500 to C L); the Capital Exemplary Research Wards Project (BCRW202001 to C L); and Tsinghua University-Peking Union Medical College Hospital Initiative Scientific Research Program (2019ZLH202 to Z L). The funders had no role in study design, data collection and analysis, decision to publish, or preparation of the manuscript.

Author contribution statement

All authors contributed to the study conception and design. Material preparation, data collection, and analysis were performed by Lanping Jiang, Xiaoyan Peng, Bingbin Zhao, Lei Zhang, and Lubin Xu. The first draft of the manuscript was written by Lanping Jiang, and the manuscript was reviewed and edited by Xiaoyan Peng, Min Nie, and Limeng Chen. All authors read and approved the final manuscript.

Acknowledgements

Portions of this study were previously presented in abstract at Annual Meeting of the American Society of Nephrology in 2012 and 2014, at 53rd ERA-EDTA in 2016. The authors are grateful to Dr Hongbin Tu from National Institutes of Health for his assistance of $^{22}\text{Na}^+$ uptake experiment and valuable suggestions.

References

- Riveira-Munoz E, Chang Q, Godefroid N, Hoenderop JG, Bindels RJ, Dahan K, Devuyst O & Belgian Network for Study of Gitelman Syndrome. Transcriptional and functional analyses of SLC12A3 mutations: new clues for the pathogenesis of Gitelman syndrome. *Journal of the American Society of Nephrology* 2007 **18** 1271–1283. (<https://doi.org/10.1681/ASN.2006101095>)
- Mastroianni N, De Fusco M, Zollo M, Arrigo G, Zuffardi O, Bettinelli A, Ballabio A & Casari G. Molecular cloning, expression pattern, and chromosomal localization of the human Na-Cl thiazide-sensitive cotransporter (SLC12A3). *Genomics* 1996 **35** 486–493. (<https://doi.org/10.1006/geno.1996.0388>)
- Ma J, Ren H, Lin L, Zhang C, Wang Z, Xie J, Shen PY, Zhang W, Wang W, Chen XN, *et al.* Genetic features of Chinese patients with Gitelman syndrome: sixteen novel SLC12A3 mutations identified in a new cohort. *American Journal of Nephrology* 2016 **44** 113–121. (<https://doi.org/10.1159/000447366>)
- Wang F, Shi C, Cui Y, Li C & Tong A. Mutation profile and treatment of Gitelman syndrome in Chinese patients. *Clinical and Experimental Nephrology* 2017 **21** 293–299. (<https://doi.org/10.1007/s10157-016-1284-6>)
- Vargas-Poussou R, Dahan K, Kahila D, Venisse A, Riveira-Munoz E, Debaix H, Grisart B, Bridoux F, Unwin R, Moulin B, *et al.* Spectrum of mutations in Gitelman syndrome. *Journal of the American Society of Nephrology* 2011 **22** 693–703. (<https://doi.org/10.1681/ASN.2010090907>)
- Tseng MH, Yang SS, Hsu YJ, Fang YW, Wu CJ, Tsai JD, Hwang DY & Lin SH. Genotype, phenotype, and follow-up in Taiwanese patients with salt-losing tubulopathy associated with SLC12A3 mutation. *Journal of Clinical Endocrinology and Metabolism* 2012 **97** E1478–E1482. (<https://doi.org/10.1210/jc.2012-1707>)
- Glaudemans B, Yntema HG, San-Cristobal P, Schoots J, Pfundt R, Kamsteeg EJ, Bindels RJ, Knoers NV, Hoenderop JG & Hoefsloot LH. Novel NCC mutants and functional analysis in a new cohort of patients with Gitelman syndrome. *European Journal of Human Genetics* 2012 **20** 263–270. (<https://doi.org/10.1038/ejhg.2011.189>)
- Maki N, Komatsuda A, Wakui H, Ohtani H, Kigawa A, Aiba N, Hamai K, Motegi M, Yamaguchi A, Imai H, *et al.* Four novel mutations in the thiazide-sensitive Na-Cl co-transporter gene in Japanese patients with Gitelman's syndrome. *Nephrology, Dialysis, Transplantation* 2004 **19** 1761–1766. (<https://doi.org/10.1093/ndt/gfh239>)
- Fujimura J, Nozu K, Yamamura T, Minamikawa S, Nakanishi K, Horinouchi T, Nagano C, Sakakibara N, Nakanishi K, Shima Y, *et al.* Clinical and genetic characteristics in patients with Gitelman syndrome. *Kidney International Reports* 2019 **4** 119–125. (<https://doi.org/10.1016/j.ekir.2018.09.015>)
- Qin L, Shao L, Ren H, Wang W, Pan X, Zhang W, Wang Z, Shen P & Chen N. Identification of five novel variants in the thiazide-sensitive NaCl co-transporter gene in Chinese patients with Gitelman syndrome. *Nephrology* 2009 **14** 52–58. (<https://doi.org/10.1111/j.1440-1797.2008.01042.x>)
- Zeng Y, Li P, Fang S, Wu C, Zhang Y, Lin X & Guan M. Genetic analysis of SLC12A3 gene in Chinese patients with Gitelman syndrome. *Medical Science Monitor* 2019 **25** 5942–5952. (<https://doi.org/10.12659/MSM.916069>)
- Jiang L, Chen C, Yuan T, Qin Y, Hu M, Li X, Xing X, Lee X, Nie M & Chen L. Clinical severity of Gitelman syndrome determined by serum magnesium. *American Journal of Nephrology* 2014 **39** 357–366. (<https://doi.org/10.1159/000360773>)
- Jiang L, Peng X, Ma J, Yuan T, Qin Y, Wang O, Wang H, Wang Y, Chen G, Yue C, *et al.* Normomagnesemic Gitelman syndrome patients exhibit a stronger reaction to thiazide than hypomagnesemic patients. *Endocrine Practice* 2015 **21** 1017–1025. (<https://doi.org/10.4158/EP14432.OR>)
- Peng XY, Jiang LP, Yuan T, Yue C, Zheng K, Wang O, Li NS, Li W, Tong AL, Xing XP, *et al.* Value of chloride clearance test in differential diagnosis of Gitelman syndrome. *Zhongguo Yi Xue Ke Xue Yuan Xue Bao* 2016 **38** 275–282. (<https://doi.org/10.3881/j.issn.1000-503X.2016.03.006>)
- Peng X, Jiang L, Chen C, Qin Y, Yuan T, Wang O, Xing X, Li X, Nie M & Chen L. Increased urinary prostaglandin E2 metabolite: a potential therapeutic target of Gitelman syndrome. *PLoS ONE* 2017 **12** e0180811. (<https://doi.org/10.1371/journal.pone.0180811>)
- Yuan T, Jiang L, Chen C, Peng X, Nie M, Li X, Xing X, Li X & Chen L. Glucose tolerance and insulin responsiveness in Gitelman syndrome patients. *Endocrine Connections* 2017 **6** 243–252. (<https://doi.org/10.1530/EC-17-0014>)

- 17 Peng X, Zhao B, Zhang L, Jiang L, Yuan T, Wang Y, Wang H, Ma J, Li N, Zheng K, *et al.* Hydrochlorothiazide test as a tool in the diagnosis of Gitelman syndrome in Chinese patients. *Frontiers in Endocrinology* 2018 **9** 559. (<https://doi.org/10.3389/fendo.2018.00559>)
- 18 Jiang L. *Establishment of Gitelman Syndrome's Diagnosis Methods and A Preliminary Study of Vitamin D's Inhibition Mechanism on Renin Activation*. PhD Thesis, Peking Union Medical College Hospital, Peking Union Medical College, Chinese Academy of Medical Sciences, 2015.
- 19 De Jong JC, Van Der Vliet WA, Van Den Heuvel LP, Willems PH, Knoers NV & Bindels RJ. Functional expression of mutations in the human NaCl cotransporter: evidence for impaired routing mechanisms in Gitelman's syndrome. *Journal of the American Society of Nephrology* 2002 **13** 1442–1448. (<https://doi.org/10.1097/01.asn.0000017904.77985.03>)
- 20 Kunchaparty S, Palco M, Berkman J, Velazquez H, Desir GV, Bernstein P, Reilly RF & Ellison DH. Defective processing and expression of thiazide-sensitive Na-Cl cotransporter as a cause of Gitelman's syndrome. *American Journal of Physiology* 1999 **277** F643–F649. (<https://doi.org/10.1152/ajprenal.1999.277.4.F643>)
- 21 Sabath E, Meade P, Berkman J, de los Heros P, Moreno E, Bobadilla NA, Vazquez N, Ellison DH & Gamba G. Pathophysiology of functional mutations of the thiazide-sensitive Na-Cl cotransporter in Gitelman disease. *American Journal of Physiology: Renal Physiology* 2004 **287** F195–F203. (<https://doi.org/10.1152/ajprenal.00044.2004>)
- 22 Moreno E, Tovar-Palacio C, de los Heros P, Guzman B, Bobadilla NA, Vazquez N, Riccardi D, Poch E & Gamba G. A single nucleotide polymorphism alters the activity of the renal Na⁺:Cl⁻ cotransporter and reveals a role for transmembrane segment 4 in chloride and thiazide affinity. *Journal of Biological Chemistry* 2004 **279** 16553–16560. (<https://doi.org/10.1074/jbc.M400602200>)
- 23 Monroy A, Plata C, Hebert SC & Gamba G. Characterization of the thiazide-sensitive Na⁽⁺⁾-Cl⁽⁻⁾ cotransporter: a new model for ions and diuretics interaction. *American Journal of Physiology: Renal Physiology* 2000 **279** F161–F169. (<https://doi.org/10.1152/ajprenal.2000.279.1.F161>)
- 24 Yang SS, Fang YW, Tseng MH, Chu PY, Yu IS, Wu HC, Lin SW, Chau T, Uchida S, Sasaki S, *et al.* Phosphorylation regulates NCC stability and transporter activity in vivo. *Journal of the American Society of Nephrology* 2013 **24** 1587–1597. (<https://doi.org/10.1681/ASN.2012070742>)
- 25 Yang SS, Lo YF, Yu IS, Lin SW, Chang TH, Hsu YJ, Chao TK, Sytwu HK, Uchida S, Sasaki S, *et al.* Generation and analysis of the thiazide-sensitive Na⁺-Cl⁻ cotransporter (Ncc/Slc12a3) Ser707X knockin mouse as a model of Gitelman syndrome. *Human Mutation* 2010 **31** 1304–1315. (<https://doi.org/10.1002/humu.21364>)
- 26 Colussi G, Bettinelli A, Tedeschi S, De Ferrari ME, Syren ML, Borsa N, Mattiello C, Casari G & Bianchetti MG. A thiazide test for the diagnosis of renal tubular hypokalemic disorders. *Clinical Journal of the American Society of Nephrology* 2007 **2** 454–460. (<https://doi.org/10.2215/CJN.02950906>)
- 27 Colussi G, Rombola G, Brunati C & De Ferrari ME. Abnormal reabsorption of Na⁺/Cl⁻ by the thiazide-inhibitable transporter of the distal convoluted tubule in Gitelman's syndrome. *American Journal of Nephrology* 1997 **17** 103–111. (<https://doi.org/10.1159/000169082>)
- 28 Zhang C, Freddolino PL & Zhang Y. COFACTOR: improved protein function prediction by combining structure, sequence and protein-protein interaction information. *Nucleic Acids Research* 2017 **45** W291–W299. (<https://doi.org/10.1093/nar/gkx366>)
- 29 Yang J & Zhang Y. I-TASSER server: new development for protein structure and function predictions. *Nucleic Acids Research* 2015 **43** W174–W181. (<https://doi.org/10.1093/nar/gkv342>)
- 30 Tu H, Li H, Wang Y, Niyayati M, Wang Y, Leshin J & Levine M. Low red blood cell vitamin C concentrations induce red blood cell fragility: a link to diabetes via glucose, glucose transporters, and dehydroascorbic acid. *EBioMedicine* 2015 **2** 1735–1750. (<https://doi.org/10.1016/j.ebiom.2015.09.049>)
- 31 Amir Shaghaghi M, Zhouyao H, Tu H, El-Gabalawy H, Crow GH, Levine M, Bernstein CN & Eck P. The SLC2A14 gene, encoding the novel glucose/dehydroascorbate transporter GLUT14, is associated with inflammatory bowel disease. *American Journal of Clinical Nutrition* 2017 **106** 1508–1513. (<https://doi.org/10.3945/ajcn.116.147603>)
- 32 Corpe CJ, Tu H, Eck P, Wang J, Faulhaber-Walter R, Schnermann J, Margolis S, Padayatty S, Sun H, Wang Y, *et al.* Vitamin C transporter Slc23a1 links renal reabsorption, vitamin C tissue accumulation, and perinatal survival in mice. *Journal of Clinical Investigation* 2010 **120** 1069–1083. (<https://doi.org/10.1172/JCI39191>)
- 33 Soreq H & Seidman S. Xenopus oocyte microinjection: from gene to protein. *Methods in Enzymology* 1992 **207** 225–265. ([https://doi.org/10.1016/0076-6879\(92\)07016-h](https://doi.org/10.1016/0076-6879(92)07016-h))
- 34 Ji W, Foo JN, O'Roak BJ, Zhao H, Larson MG, Simon DB, Newton-Cheh C, State MW, Levy D & Lifton RP. Rare independent mutations in renal salt handling genes contribute to blood pressure variation. *Nature Genetics* 2008 **40** 592–599. (<https://doi.org/10.1038/ng.118>)
- 35 Lin SH, Shiang JC, Huang CC, Yang SS, Hsu YJ & Cheng CJ. Phenotype and genotype analysis in Chinese patients with Gitelman's syndrome. *Journal of Clinical Endocrinology and Metabolism* 2005 **90** 2500–2507. (<https://doi.org/10.1210/jc.2004-1905>)
- 36 Joo KW, Lee JW, Jang HR, Heo NJ, Jeon US, Oh YK, Lim CS, Na KY, Kim J, Cheong HI, *et al.* Reduced urinary excretion of thiazide-sensitive Na-Cl cotransporter in Gitelman syndrome: preliminary data. *American Journal of Kidney Diseases* 2007 **50** 765–773. (<https://doi.org/10.1053/j.ajkd.2007.07.022>)
- 37 Tsukamoto T, Kobayashi T, Kawamoto K, Fukase M & Chihara K. Possible discrimination of Gitelman's syndrome from Bartter's syndrome by renal clearance study: report of two cases. *American Journal of Kidney Diseases* 1995 **25** 637–641. ([https://doi.org/10.1016/0272-6386\(95\)90137-x](https://doi.org/10.1016/0272-6386(95)90137-x))
- 38 Zhang J, Chen Q, Li Y, Du M, Ma H, Chen H & Guo S. Utilization of furosemide/hydrochlorothiazide load test in differential diagnosis of Bartter syndrome from Gitelman syndrome in children. *Journal of Clinical Pediatrics* 2016 **34** 891–893. (<https://doi.org/10.3969/j.issn.1000-3606.2016.12.003>)
- 39 Lin SH, Cheng NL, Hsu YJ & Halperin ML. Intrafamilial phenotype variability in patients with Gitelman syndrome having the same mutations in their thiazide-sensitive sodium/chloride cotransporter. *American Journal of Kidney Diseases* 2004 **43** 304–312. (<https://doi.org/10.1053/j.ajkd.2003.10.018>)
- 40 Shao L, Lang Y, Wang Y, Gao Y, Zhang W, Niu H, Liu S & Chen N. High-frequency variant p.T60M in NaCl cotransporter and blood pressure variability in Han Chinese. *American Journal of Nephrology* 2012 **35** 515–519. (<https://doi.org/10.1159/000339165>)
- 41 Liu T, Wang C, Lu J, Zhao X, Lang Y & Shao L. Genotype/phenotype analysis in 67 Chinese patients with Gitelman's syndrome. *American Journal of Nephrology* 2016 **44** 159–168. (<https://doi.org/10.1159/000448694>)

Received in final form 16 November 2021

Accepted 3 December 2021

Accepted Manuscript published online 3 December 2021